

polarity our calculation is applicable independently of the way in which the nucleus becomes deexcited. In particular, our calculation can be applied to electrodisintegration processes such as that occurring in the giant resonance transition. This will also apply to the case of quasielastic scattering or pion electroproduction where only the scattered electrons are detected, as in that case there should be no interference between different multipoles.<sup>17</sup> However, if any of the products

<sup>17</sup> W. C. Barber, F. Berthold, G. Fricke, and F. E. Gudden, Phys. Rev. **120**, 2081 (1960). See Ref. 21 to G. Kramer in this reference.

of electrodisintegration is detected, then the problem must be studied in greater detail.

#### ACKNOWLEDGMENTS

We wish to thank J. E. Leiss, U. Fano, and V. Gillet for helpful discussions, and R. A. Schrack for help with the computer calculations. One of us (L.C.M.) wishes to thank the Physics Division of the Aspen Institute for Humanistic Studies for hospitality extended while part of this work was being completed.

## Nuclear Structure Studies in Tellurium Isotopes with $(d,p)$ and $(d,t)$ Reactions\*

R. K. JOLLY†

*University of Pittsburgh, Pittsburgh, Pennsylvania*

(Received 9 June 1964)

Shell-model states in the isotopes 123, 124, 125, 126, 127, 129, and 131 of Te have been investigated via  $(d,p)$  and  $(d,t)$  reactions with a typical resolution of 40 keV. Distorted-wave Born approximation calculations were used for the identification of the orbital angular momentum of the captured neutron in  $(d,p)$  reactions. The  $11/2^-$ ,  $3/2^+$  and  $1/2^+$  neutron subshells in the 50–82 neutron shell are found to be filling in these isotopes, although the  $3/2^+$  and  $1/2^+$  subshells are not filling as rapidly as one would normally expect. There is also found some indication of the  $7/2^-$  and the  $3/2^-$  subshells from the next major shell filling in the heaviest isotopes. The  $3/2^+$  single-particle state is found to lie the lowest in the isotopes 131 and 129, while  $11/2^-$  and  $1/2^+$  are found to lie the lowest in the isotopes 127 and 125, respectively. Single-particle energies have been calculated using pairing theory.

### I. INTRODUCTORY—EXPERIMENTAL PROCEDURE

ACCORDING to the shell-model theory<sup>1</sup> the neutron single-particle states are practically unaffected by the proton number as long as it is even. One, therefore, hopes to see about similar spectra of neutron states in neighboring isotones. Previous work of Cohen and Price<sup>2</sup> and some present work of Schneid, Prakash, and Cohen<sup>3</sup> with Sn isotopes has revealed a simple level structure of their neutron states which makes these isotopes very suitable for shell model studies via  $(d,p)$  and  $(d,t)$  reactions. From the aforesaid remark about proton number, Te isotopes (which have only two more protons than the Sn isotopes) should show a structure similar to the Sn isotopes and are, therefore, very suitable for shell-model studies in the mass region  $A \sim 125$ .

Te isotopes 124, 125, 126, 128, and 130 were deposited by vacuum evaporation on gold foils ( $\sim 0.2$  mg/cm<sup>2</sup>) to thicknesses varying from 0.5 to 1 mg/cm<sup>2</sup>. The thickness

of these targets may be uncertain by  $\sim 10\%$  at the most. These isotopes were bombarded with 14.8-MeV deuterons from the University of Pittsburgh 47-in. fixed-frequency cyclotron. The reaction products were analyzed by a 60° wedge magnet spectrograph and detected in nuclear emulsion plates. Other details of the experimental method have been described previously.<sup>4</sup>

At the time this experiment was done, it was believed from the previous work of Cohen and Price<sup>2</sup> that measurement of a complete angular distribution in  $(d,p)$  reactions is no more helpful than cross-section measurements at a few key angles judiciously chosen to give information about  $l_n$ , the orbital angular momentum of the captured neutron. In the same work it was realized that  $(d,t)$  angular distributions are much less useful, as these were found to be relatively insensitive to differences in angular momenta as compared to  $(d,p)$  angular distributions. Hence data were taken at 9, 17, 20, 30, 39, and 50 deg for  $(d,p)$  reactions and only at 45 and 60 deg for  $(d,t)$  reactions. The former choice was made by an examination of the  $(d,p)$  angular distributions for the Sn isotopes from the work of Cohen and Price<sup>2</sup> while the

\* Work supported by the National Science Foundation.

† On Research Fellowship from Panjab University, Chandigarh, India.

<sup>1</sup> M. Meyer and J. H. D. Jensen, *Elementary Theory of Nuclear Shell Structure* (John Wiley & Sons, Inc., New York, 1955).

<sup>2</sup> B. L. Cohen and R. E. Price, Phys. Rev. **121**, 1441 (1961).

<sup>3</sup> E. Schneid, A. Prakash, and B. L. Cohen (to be published).

<sup>4</sup> B. L. Cohen, R. H. Fulmer, and A. L. McCarthy, Phys. Rev. **126**, 698 (1962).

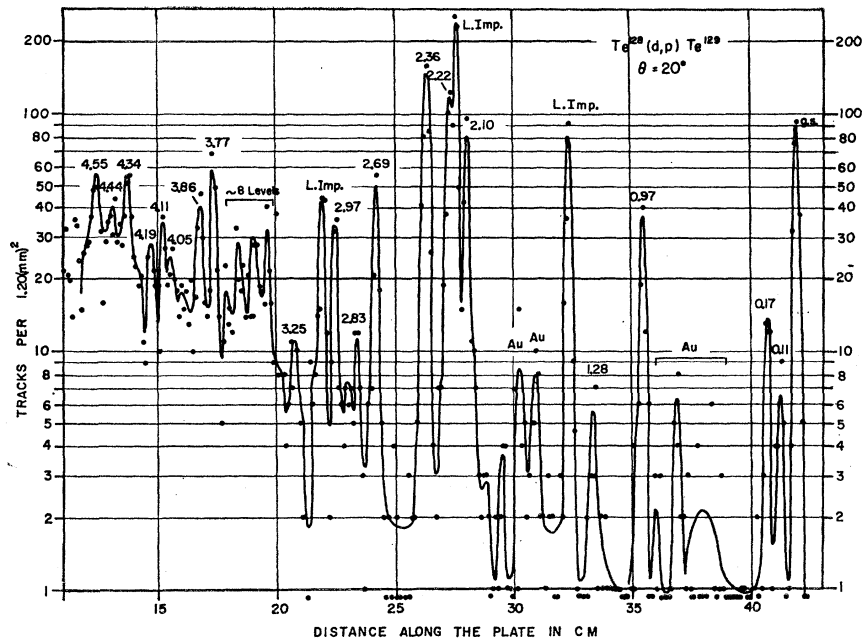


FIG. 1. Proton spectrum from the  $(d,p)$  reactions on  $\text{Te}^{128}$ . The plot is intensity versus distance along the nuclear emulsion plate. The numbers that appear on the intensity peaks are the excitation energies of the states of the residual nucleus measured from the ground state.  $\theta$  is the scattering angle at which the spectrum was taken. The intensity peaks marked Au are from the Au backing of the  $\text{Te}^{128}$  target.

latter was a happy compromise between too heavy a deuteron background (as deuterons and tritons overlap towards the low-energy end of the triton spectrum. In proton spectra the problem of overlapping spectra is resolved by use of an absorber thick enough to stop everything except the protons) and too low a cross section. It has recently been realized that extension of both  $(d,p)^5$  and  $(d,t)^6$  angular distributions to angles

larger than  $90^\circ$  is helpful in spin assignments particularly for the case  $l_n=1$ . However, the ambiguous cases of spin assignments in the present work were few as compared to the entire mass of useful spectroscopic data obtained from the present work.

To separate the deuteron and the triton groups in the region of interference, inelastic deuteron scattering was done for all the Te isotopes investigated in this work. Triton and deuteron spectra were always taken at two angles to single out the groups due to light contaminants in the targets. Typical  $(d,p)$  and  $(d,t)$  reaction spectra leading to the states of  $\text{Te}^{129}$  are shown in Figs. 1 and 2, respectively.

## II. ANALYSIS OF THE DATA (GENERAL)

### A. Spin and Parity Assignments

The angular distribution data were analyzed with direct reaction theory using the distorted-wave Born approximation (DWBA) calculations of Satchler *et al.*<sup>7</sup> The input proton and deuteron optical model parameters were the average parameters of Perey and Perey<sup>8</sup> and are as follows:

*Deuterons:*

$$V=98.3, \quad r_0=1.15, \quad a=0.81, \quad r_{0c}=1.3, \\ W'=61, \quad r'_0=1.34, \quad a'=0.68,$$

$$\text{Protons: } V=53, \quad r_0=1.25, \quad a=0.65, \quad r_{0c}=1.25, \\ W'=42, \quad r'_0=1.25, \quad a'=0.47,$$

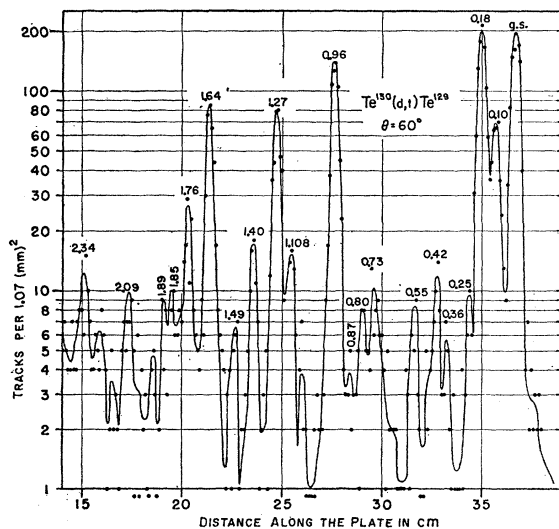


FIG. 2. Triton spectrum from the  $(d,t)$  reactions on  $\text{Te}^{130}$ . See also the caption for Fig. 1.

<sup>5</sup> J. P. Schiffer, Proceedings of the Conference on Nuclear Spectroscopy with Direct Interactions held in Chicago, 9-11 March 1964 (unpublished).

<sup>6</sup> R. H. Fulmer and W. W. Daehnick, Proceedings of the Conference on Nuclear Spectroscopy with Direct Interactions held in Chicago, 9-11 March 1964 (unpublished).

<sup>7</sup> R. H. Bassel, R. M. Drisko, and G. R. Satchler, Oak Ridge National Laboratory Report No. ORNL-3240 (Physics) (unpublished).

<sup>8</sup> C. M. Perey and F. G. Perey, Phys. Rev. **132**, 755 (1963); F. G. Perey, *ibid.* **131**, 745 (1963).

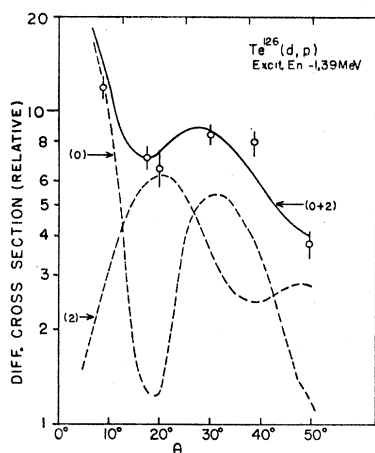


FIG. 3.  $l_n=0$  and  $l_n=2$  theoretical angular distributions are appropriately mixed to fit the experimental angular distribution of the proton group from  $\text{Te}^{126}(d,p)$  reactions leading to the 1.39 MeV state of  $\text{Te}^{127}$ .

where the notation and the units ( $V, W$  in MeV;  $r, a$  in F) are those used in Ref. 7. A lower cutoff of 7.51 F was used although slightly different cutoffs did not seem to make much difference. Not using a lower cutoff was found to affect the angular distributions drastically, particularly those for small values of  $l_n$ , the orbital angular momentum of the captured neutron. An upper cutoff of 3 times the nuclear radius was usually employed except in cases of negative reaction  $Q$  values where even larger upper cutoffs ( $\sim 5$  times the nuclear radius) were found unsatisfactory for small angles ( $< 30^\circ$ ). This was particularly noticeable in the angular distributions of  $l_n=0$  and 1.

The theoretical angular distributions thus obtained were found very useful in  $l_n$  determinations as the distributions for the different orbital angular momenta are fairly distinct at least for small angular momenta, and the shape agreement with the experimental distributions for isolated and unmixed transitions was very good. In the case of overlapping levels an appropriate "mixture" of the theoretical angular distributions was taken to fit the experimental angular distributions. An example of this procedure is shown in Fig. 3. The relative strength of the mixed transitions was very uncertain if the corresponding angular momenta were widely different as for example in mixing the angular distributions of  $l_n=1$  and  $l_n=5$  or 6. Using this procedure it was possible to fit the angular distributions of almost all the states. Spin assignments were then made using (i) the conventional shell-model ordering of states, i.e., the higher spin member of the  $1\cdot s$  doublet lies lower in energy than the lower spin member; (ii) the approximate magnitudes of the  $1\cdot s$  splitting obtained from Ref. 9 (Table I) and (iii) the ratio  $S_p/S_t$  of spectroscopic factors obtained from cross sections of exciting the same state via  $(d,p)$  and  $(d,t)$  reactions, respectively. This ratio should be large for a state that is more empty and relatively small for one that is more full. A

<sup>9</sup> B. L. Cohen, P. Mukherjee, R. H. Fulmer, and A. L. McCarthy, Phys. Rev. **127**, 1678 (1962).

TABLE I.  $1\cdot s$  splitting ( $\Delta E$ ) magnitudes for Te isotopes.

$l$	$\Delta E(1\cdot s)$ , MeV
1	$\sim 1$
2	$\sim 1.7$
3	$\sim 2.4$
5	$\sim 5.5$

detailed discussion of the results in different isotopes will be found in Sec. III of the text.

### B. Pairing Theory and Its Parameters

According to the theory of Kisslinger and Sorenson<sup>10</sup> and Belyaev,<sup>11</sup> the strong pairing interaction between identical nucleons causes configuration mixing between the low-lying shell-model states and as a result these states do not fill one after another but simultaneously. The fullness of the subshells (spin  $j$ ) is expressed in terms of the quantities  $V_j^2$  such that

$$(2j+1)V_j^2 = n_j, \quad (1)$$

the number of neutrons in that subshell. The emptiness of the same subshell  $U_j^2$  is defined by

$$U_j^2 + V_j^2 = 1. \quad (2)$$

The single-particle state involved in the transfer of a neutron of a given spin and parity (notation  $J^\pi$ ) is no longer single but a multiplet of states. The fullness or the emptiness of a subshell comprising this multiplet is obtained from the spectroscopic factors for the members of the multiplet. The spectroscopic factors can be extracted from the experimental cross sections in the following way. In  $(d,p)$  reactions on an even target, the spectroscopic factor for a neutron capture of spin  $j$  is

$$S_j^m = \frac{[d\sigma/d\Omega(d,p)]_m}{[d\sigma/d\Omega(d,p)]_{s.p.}} \times \frac{1}{2j+1}, \quad (3)$$

where the superscript  $m$  denotes a certain member of the multiplet which constitutes a single-particle shell model state. The numerator is the experimental differential cross section while the single-particle (s.p.) cross section is obtained from DWBA calculations. With definition (3)

$$\sum_m S_j^m \approx U_j^2. \quad (4)$$

Similar considerations hold for  $(d,t)$  reactions and fullness of a single-particle state.

In odd isotopes the quantity on the right-hand side of (3) has to be multiplied with  $2I_f+1/2I_i+1$  (see Ref.

<sup>10</sup> L. S. Kisslinger and R. A. Sorenson, Kgl. Danske Videnskab. Selskab, Mat. Fys. Medd. **32**, No. 9 (1960).

<sup>11</sup> S. T. Belyaev, Kgl. Danske Videnskab. Selskab, Mat. Fys. Medd. **31**, No. 11 (1959).

TABLE II. The occupation numbers  $U_j^2$  and  $V_j^2$  of pairing theory (Ref. 10) for the various single-particle states in the isotopes of Te studied in this work. The inequality sign ( $>$ ) before some numbers means that several members of the single-particle transition multiplet have been missed; question mark means that though the states are seen via  $(d,t)$  reactions, reliable occupation numbers cannot be extracted either due to normalization difficulties or inability to identify the spin and parity of the observed states; ellipses ( $\dots$ ) means that the corresponding states are not seen via  $(d,t)$  reactions. Other details are explained in the text.

Target A \ S.P. state	3/2 <sup>+</sup>	11/2 <sup>-</sup>	1/2 <sup>+</sup>	5/2 <sup>+</sup>	7/2 <sup>-</sup>	3/2 <sup>-</sup>	1/2 <sup>-</sup>	5/2 <sup>-</sup>	$\Sigma_j(2j+1)U_j^2$ for 11/2 <sup>-</sup> , 1/2 <sup>+</sup> and 3/2 <sup>+</sup>	Number of holes in 11/2 <sup>-</sup> , 1/2 <sup>+</sup> and 3/2 <sup>+</sup>
130 $\left\{ \begin{array}{l} U_j^2 \\ V_j^2 \end{array} \right.$	0.28 0.73	0.31 0.61	0.31 0.65	0.037 ?	>0.40 ?	>0.35 ...	>0.60 ...	>0.63 ...	5.46	4
128 $\left\{ \begin{array}{l} U_j^2 \\ V_j^2 \end{array} \right.$	0.33 0.64	0.56 0.57	0.37 0.70	0.06 ?	>0.74 ?	>0.38 ?	>0.76 ...	? ...	8.78	6
126 $\left\{ \begin{array}{l} U_j^2 \\ V_j^2 \end{array} \right.$	0.45 0.60	0.45 0.48	0.55 0.41	0.10 ?	>0.43 ...	>0.64 ...	>0.35 ...	>0.43 ...	8.30	8
125 $\left\{ \begin{array}{l} U_j^2 \\ V_j^2 \end{array} \right.$	? ?	... ...	0.16 ?	? ?	... ...	... ...	... ...	... ...	? ?	9
124 $\left\{ \begin{array}{l} U_j^2 \\ V_j^2 \end{array} \right.$	0.31 ...	... ...	0.08 ?	0.06 ?	... ...	... ...	... ...	... ...	? ?	10

12) to get the spectroscopic factors that will obey (4) for the various members of a single-particle transition multiplet. Experimentally the spectroscopic factors for  $(d,p)$  reactions are obtained as the ratio of the experimental to the theoretical cross sections using DWBA calculations as mentioned above. The experimental cross section is measured at the first maximum of the angular distribution provided it is larger than  $10^\circ$ . These angles were chosen as follows:  $l=0, 30^\circ$ ;  $l=1, 30^\circ$ ;  $l=2, 20^\circ$ ;  $l=3, 20^\circ$ ;  $l=4, 30^\circ$ ;  $l=5, 39^\circ$ ; and  $l=6, 50^\circ$ . This method is not applicable to  $(d,t)$  reactions since no realistic triton parameters are available. As a result the following method was used.  $V_j^2$  for one of the well-resolved states, e.g.,  $\frac{3}{2}^+$  in Te<sup>129</sup>, was calculated using Eq. (2) and thence the  $(d,t)$  spectroscopic factors for the states of same spin and parity were determined by the ratio of their cross sections taking into account any  $Q$  value differences by the formula (5) discussed below. The same method is repeated for other well-resolved states, e.g.,  $\frac{1}{2}^+$  in Te<sup>129</sup> until it cannot be carried any further in which case the spectroscopic factors for two states of different spin and parity can be compared using the following empirical formula of Cohen and Price,<sup>2</sup> viz:

$$[(d\sigma/d\Omega)(d,t)]_{s.p.} = k(\theta)f(l)(1.18)^Q, \quad (5)$$

where  $k(\theta)$  is a function of  $\theta$  and is therefore eliminated in comparisons of cross sections of states observed at the same angle. The functional dependence of  $(d,t)$  single-particle cross sections on  $l$  was assumed to be the same as in  $(d,p)$  reactions so that it could be determined from the DWBA calculations. To renormalize  $U_j^2$  because of inherent normalization errors in DWBA calculations, the numbers  $U_j^2$  for a certain state, e.g.,  $\frac{3}{2}^+$  were multiplied by an adjustable constant  $A$  in all the neighboring isotopes and the sum

$$AU_{3/2^2} + V_{3/2^2} = \alpha \quad (6)$$

was varied by varying  $A$  in all the isotopes until  $\alpha$  was

<sup>2</sup> B. L. Cohen and O. V. Chubinsky, Phys. Rev. **131**, 2184 (1963).

almost the same in the various isotopes. The equations (6) were then divided by the average of the set of numbers  $\alpha$  finally obtained in the process of renormalization of  $U_j^2$  and  $V_j^2$ . This process was repeated for all the states seen both in  $(d,p)$  and  $(d,t)$ . The values of  $A$  in the renormalization done in this work lay between 0.75 and 2.0. The renormalized occupation numbers are given in Table II. No attempt was made to renormalize the  $U_j^2$  for the subshells of the next major shell and one notices large deviations from the value unity expected for almost all the single-particle states except  $\frac{7}{2}^-$  and maybe  $\frac{3}{2}^-$  in the heaviest isotopes of Te. There is some explanation of the low values of  $U_j^2$  to be found in the increasing complexity of the neutron spectra with decreasing mass number going down from Te<sup>131</sup>. The observation (last two columns of Table II) that the number of holes in 11/2<sup>-</sup>,  $\frac{3}{2}^+$  and  $\frac{1}{2}^+$  is always more than expected, may be significant in that no states in the next major shell have been taken into account and that these may be slightly populated. This conclusion is also supported by the observation of some low-lying states of the next major shell in  $(d,t)$  reactions as shall be pointed out below (Sec. III).

The single-quasiparticle energies (Table III) were calculated by taking the weighted mean of the excitation energies of the members of a single-particle transition multiplet, viz.,

$$E_j = \sum_m E_j^m S_j^m / \sum_m S_j^m, \quad (6)$$

where the summation is over all the members of a multiplet. The single-particle energies  $\epsilon_j$  can be determined from these using the following result from pairing theory, viz.:

$$\Delta + E_j = [(\epsilon_j - \lambda)^2 + \Delta^2]^{1/2}, \quad (7)$$

where  $\lambda$  is the Fermi energy and  $\Delta$  is almost the energy of the lowest quasiparticle state,  $E_{g.s.}$ , relative to the vacuum and is measured from the separation energies of the last neutron in neighboring isotopes as well as

the nucleus under study using the relation

$$\Delta(n) \simeq \frac{1}{4} \{ |SE(n) - SE(n-1)| + |SE(n) - SE(n+1)| \}. \quad (8)$$

The separation energies were taken from the work of Patell.<sup>13</sup> The values of  $\lambda$  necessary for the calculation of  $\epsilon_j$ 's were taken from Kisslinger-Sorenson<sup>10</sup> calculations of these numbers for such Sn isotopes as are isotonic with the isotopes of Te studied in this work. Since their values of  $\lambda$  are found to increase monotonically with neutron number, the values of  $\lambda$  for the heaviest isotopes were obtained by extrapolation. To resolve the ambiguity of sign in the roots of Eq. (7) in determining the single-particle energies, the quasiparticle energies of the states that are filling were plotted against mass number  $A$  of the various isotopes (Fig. 4) and whether a level

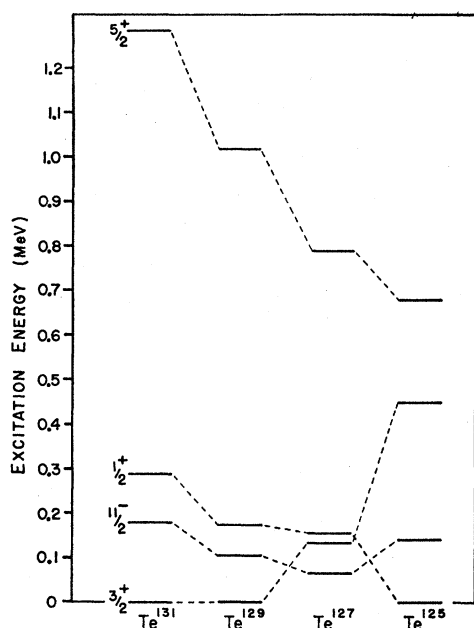


FIG. 4. The centers of gravity of the various single-quasiparticle states in the  $50 < N \leq 82$  neutron major shell are plotted for the various odd mass Te isotopes. Both  $(d,p)$  and  $(d,t)$  reaction data were used wherever possible to get the best energies of these states.

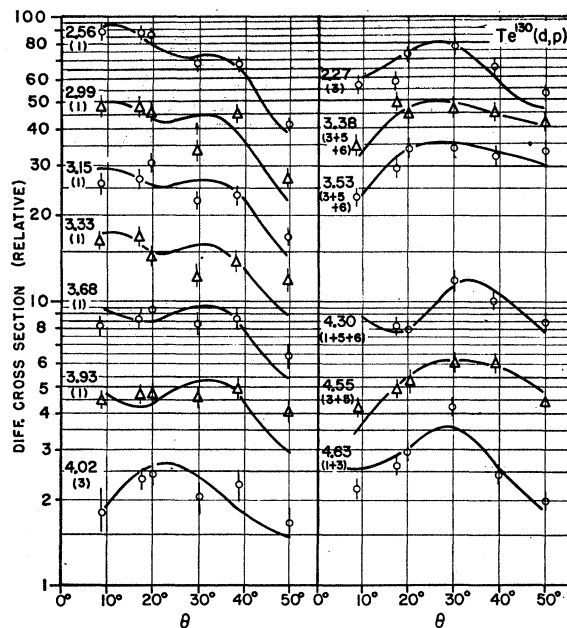
lies below or above the Fermi surface was decided by an examination of the slope  $dE_j/dA$  of these states.

### III. RESULTS AND DISCUSSION

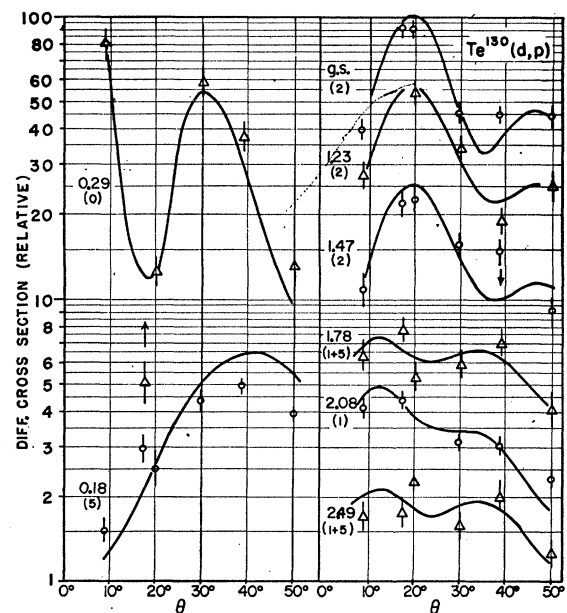
#### A. Spectroscopy of the Odd Isotopes

The experimental angular distributions and the theoretical fits to them are shown in Figs. 5-8 for the various states of  $\text{Te}^{131}$ ,  $\text{Te}^{129}$ ,  $\text{Te}^{127}$ , and  $\text{Te}^{125}$  nuclei. The quality of fits in unmixed transitions was good enough to encourage a wide use of mixtures of these angular distributions to isolate the components of

<sup>13</sup> Roshan Patell, M.S. thesis, University of Pittsburgh, 1963 (unpublished).

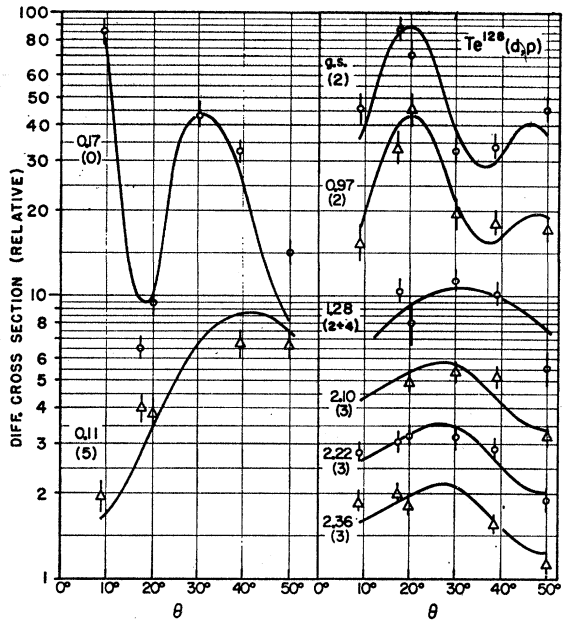


(a)

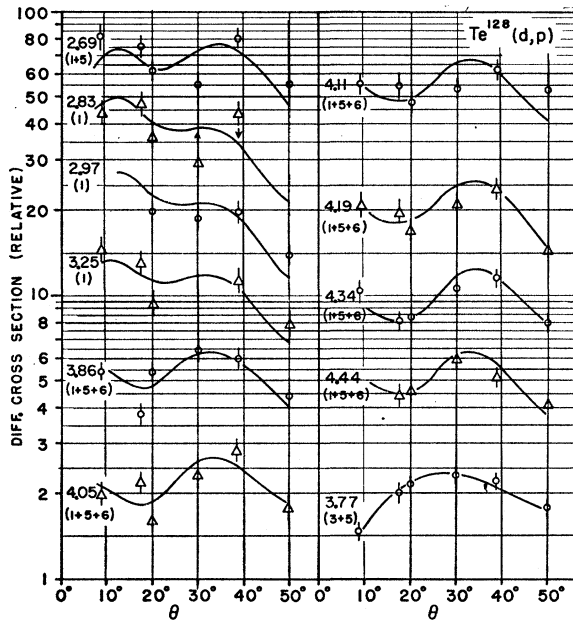


(b)

FIG. 5. (a) and (b) Angular distributions of the proton groups leading to the states of  $\text{Te}^{131}$ . The continuous curves going through the points are the DWBA calculations while the points are relative experimental cross sections. The numbers on the left of the angular distributions are excitation energies and orbital angular momentum of the captured neutron (within parentheses). In some cases the theoretical distributions for different angular momenta of the captured neutron had to be added to fit the experimental points. This fact is indicated by putting a plus sign between the orbital angular momenta noted within parentheses. In the cases marked  $(3+5+6)$  or  $(1+5+6)$  the author could not distinguish between appropriate mixtures of 5 or 6 to 3 and 1, respectively, and hence took their average. The separation of the figure into parts (a) and (b) is only for convenience in presentation.



(a)

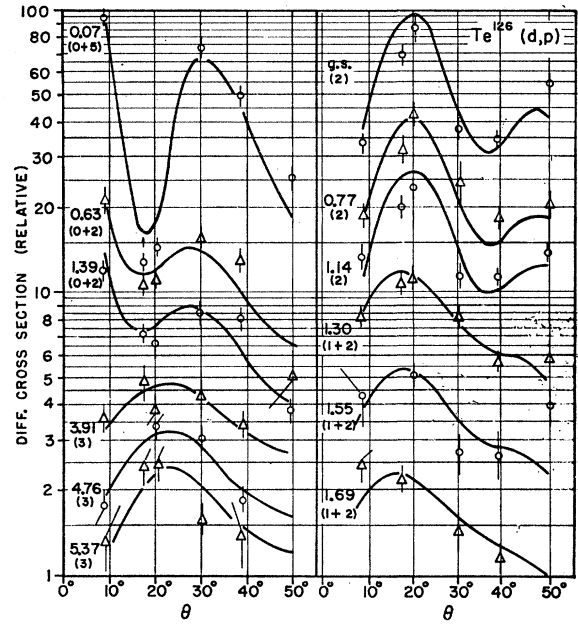


(b)

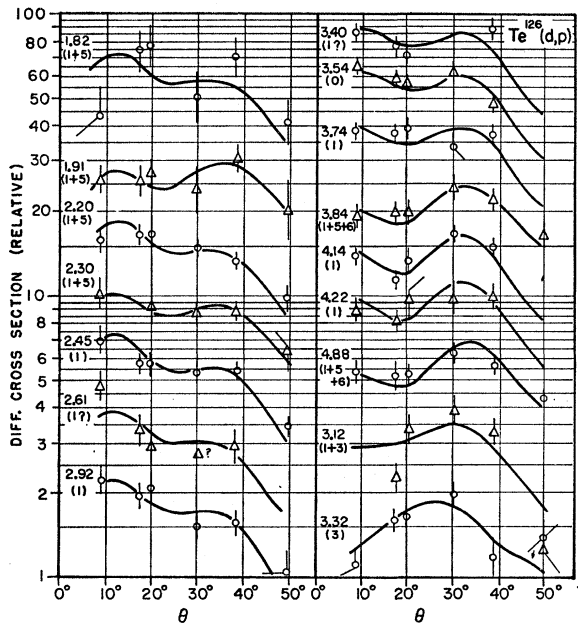
FIG. 6. (a) and (b) Angular distributions of the proton groups leading to the states of  $Te^{129}$ . See also the caption for Fig. 5.

interfering transitions. The results for the various states of these isotopes are listed in Tables IV-VII. Some states of  $Te^{129}$ ,  $Te^{127}$ , and  $Te^{125}$  were also observed in  $(d,t)$  reactions and the information from these was used to complement that from  $(d,p)$  reactions. The results of analyses of these reactions are given in Tables IX-XI. The spin assignments in these tables are taken either from  $(d,p)$  data or from some previous work

whose reference is given in these tables. The spin assignments to states in the first major shell are unambiguous except for  $l_n=2$ . In this case  $\frac{5}{2}^+$  is believed to be mostly full and one does not expect  $\frac{5}{2}^+$  states to appear very prominently in the high-energy part of the spectra. The support in favor of the assignments  $\frac{5}{2}^+$  comes from (i) Fig. 4 where the  $\frac{5}{2}^+$  is seen as one lying below the Fermi surface while the  $\frac{3}{2}^+$  is either on or slightly above the surface ( $Te^{125}$ ); (ii) the fact that  $\frac{7}{2}^+$



(a)



(b)

FIG. 7. (a) and (b) Angular distributions of the proton groups leading to the states of  $Te^{127}$ . See also the caption for Fig. 5.

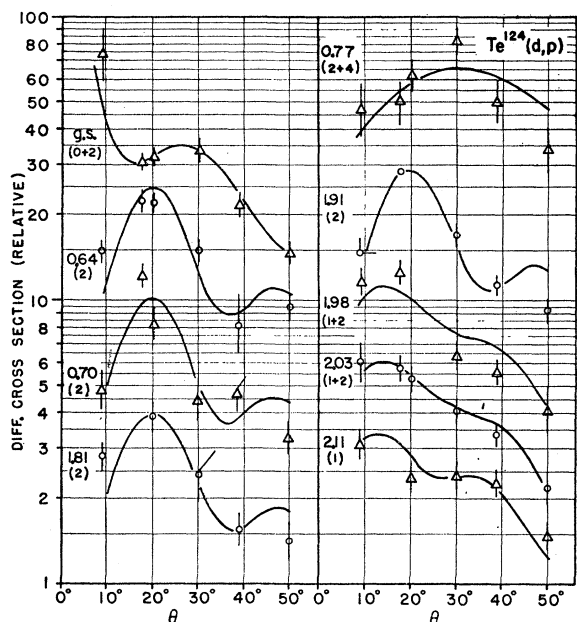


FIG. 8. Angular distributions of the proton groups leading to the states of Te<sup>128</sup>. See also the caption for Fig. 5.

being mostly full should give a ratio  $S_p/S_t$  which is greater than that for  $\frac{3}{2}^+$  (at least in the lighter isotopes where  $\frac{3}{2}^+$  cannot be as full as  $\frac{5}{2}^+$ ) and that this is borne out by the values of this ratio listed in the Tables V-VII.

States of Te<sup>123</sup> were investigated only by (d,t) reactions. A summary of the results of the analyses on the odd isotopes is given in Fig. 9. One feature which is immediately obvious from this figure is that the splitting of the quasiparticle states increases as one goes to lighter isotopes. This leads to a greater density of states and smaller cross sections for individual transitions both of which tend to make the analysis difficult.

TABLE III. The centers of gravity,  $E_j$ , of the observed states of the same spin and parity, the single-particle (s.p.) energies  $\epsilon_j$  and the parameters  $\lambda$  and  $\Delta$  of pairing theory for the various isotopes of Te studied in this work. The details of calculating these numbers are explained in the text. All energies are in MeV.

Te <sup>131</sup>				Te <sup>127</sup>					
S.P. state	$E_j$	$\epsilon_j$	$\Delta$	$\lambda$	S.P. state	$E_j$	$\epsilon_j$	$\Delta$	$\lambda$
3/2 <sup>+</sup>	0.0	3.84	1.20	3.84	3/2 <sup>+</sup>	0.14	4.00	1.40	3.36
11/2 <sup>-</sup>	0.18	3.16			11/2 <sup>-</sup>	0.07	2.92		
1/2 <sup>+</sup>	0.29	2.95			1/2 <sup>+</sup>	0.16	2.67		
5/2 <sup>+</sup>	1.28	1.67			5/2 <sup>+</sup>	0.79	1.68		
7/2 <sup>-</sup>	2.27	7.09			7/2 <sup>-</sup>	2.40	6.89		
3/2 <sup>-</sup>	2.70	7.56			3/2 <sup>-</sup>	2.85	7.37		
1/2 <sup>-</sup>	4.00	8.90			1/2 <sup>-</sup>	4.42	9.01		
5/2 <sup>-</sup>	>4.10	>9.00			5/2 <sup>-</sup>	>5.00	>9.60		
9/2 <sup>-</sup>	>3.58	>8.45			13/2 <sup>+</sup>	>4.30	>8.88		
13/2 <sup>+</sup>	>3.75	>8.64			9/2 <sup>-</sup>	>2.64	>7.15		
Te <sup>129</sup>				Te <sup>125</sup>					
3/2 <sup>+</sup>	0.00	3.60	1.32	3.60	1/2 <sup>+</sup>	0.00	3.12	1.36	3.12
11/2 <sup>-</sup>	0.11	3.04			3/2 <sup>+</sup>	0.45	4.31		
1/2 <sup>+</sup>	0.17	2.91			5/2 <sup>+</sup>	0.65	1.64		
5/2 <sup>+</sup>	1.02	1.67							
7/2 <sup>-</sup>	2.25	6.92							
3/2 <sup>-</sup>	2.98	7.69							
1/2 <sup>-</sup>	4.22	8.97							
5/2 <sup>-</sup>	>3.77	>8.51							
13/2 <sup>+</sup>	>4.23	>8.99							

TABLE IV. Spectroscopic data from Te<sup>130</sup>(d,p)Te<sup>131</sup> reactions. The details of obtaining these data are described in the text. Parentheses imply probability rather than certainty. Bracketed rows refer to an unresolved group of states whose angular distribution has been simulated by an appropriate mixture of angular distributions of the bracketed angular momenta. In the case of three bracketed angular momenta, it was impossible to distinguish between a certain mixture involving  $l_n=5$  and another involving  $l_n=6$  and hence an average of the two mixtures involving both  $l_n=5$  and  $l_n=6$  was taken to fit the experimental angular distribution.

Excit. energy (MeV)	$l_n$	$J^\pi$	$\sigma(\theta_0)$ (mb/sr)	$S_p$	Known (Ref. 14)	
					Excit. energy	$J^\pi$
0.00	2	3/2 <sup>+</sup>	1.84	0.28	0	(3/2 <sup>+</sup> )
0.18	(5)	(11/2 <sup>-</sup> )	0.23	0.31	0.182	(11/2 <sup>-</sup> )
0.29	0	1/2 <sup>+</sup>	1.32	0.31		
1.22	2	(5/2 <sup>+</sup> )	0.39	0.029		
1.46	2	(5/2 <sup>+</sup> )	0.15	0.010		
1.78	{(1) (5)}	(3/2 <sup>-</sup> )	0.17	{0.13 0.054}		
2.08	1	(3/2 <sup>-</sup> )	0.14	0.10		
2.27	3	7/2 <sup>-</sup>	4.19	0.40		
2.37	?	...	0.07	...		
2.49	{(1) (5)}	(3/2 <sup>-</sup> )	0.52	{0.45 0.11}		{0.032 0.074}
2.56	1	(3/2 <sup>-</sup> )	2.52	0.18		
2.99	1	(3/2 <sup>-</sup> )	0.98	0.064		
3.15	1	(3/2 <sup>-</sup> )	0.63	0.039		
3.33	1	(3/2 <sup>-</sup> )	0.33	0.020		
3.38	{(3) (5) (6)}	(9/2 <sup>-</sup> ) (13/2 <sup>+</sup> )	0.69	{0.59 0.15 0.18}		{0.051 0.078 0.19}
3.53	{(3) (5) (6)}	(5/2 <sup>-</sup> ) (9/2 <sup>-</sup> ) (13/2 <sup>+</sup> )	1.47	{1.25 0.33 0.38}		{0.10 0.17 0.40}
3.68	1	(1/2 <sup>-</sup> )	1.99	0.25		
3.93	1	(1/2 <sup>-</sup> )	0.88	0.10		
4.02	3	(5/2 <sup>-</sup> )	2.24	0.17		
4.30	{(1) (5) (6)}	(1/2 <sup>-</sup> ) (9/2 <sup>-</sup> ) (13/2 <sup>+</sup> )	2.02	{1.67 0.29 0.26}		{0.20 0.12 0.25}
4.55	{(3) (5)}	(5/2 <sup>-</sup> ) (9/2 <sup>-</sup> )	2.52	{1.94 1.59}		{0.12 0.61}
4.63	{(1) (3)}	(1/2 <sup>-</sup> ) (5/2 <sup>-</sup> )	2.36	{0.42 0.13}		{0.054 0.13}

TABLE V. Spectroscopic data from Te<sup>128</sup>(d,p)Te<sup>129</sup> reactions. See also the caption for Table IV.

Excit. energy (MeV)	$l_n$	$J^\pi$	$\sigma(\theta_0)$ (mb/sr)	$S_p$	Known (Ref. 14)		
					Excit. energy	$J^\pi$	$S_p/S_t$
0.00	2	3/2 <sup>+</sup>	2.00	0.33	0	(3/2 <sup>+</sup> )	0.45
0.11	(5)	(11/2 <sup>-</sup> )	0.40	0.56	0.106	(11/2 <sup>-</sup> )	
0.17	0	1/2 <sup>+</sup>	1.56	0.37			
0.97	2	(5/2 <sup>+</sup> )	0.66	0.056			0.20
1.28	{(2) (4)}	(5/2 <sup>+</sup> ) (7/2 <sup>+</sup> )	0.20	{0.13 0.13}			
2.10	3	(7/2 <sup>-</sup> )	1.65	0.18			
2.22	3	(7/2 <sup>-</sup> )	2.40	0.25			
2.36	3	(7/2 <sup>-</sup> )	3.10	0.31			
2.69	{(1) (5)}	(3/2 <sup>-</sup> ) (9/2 <sup>-</sup> )	0.81	{0.52 0.40}			
2.83	1	3/2 <sup>-</sup>	2.30	0.16			
2.97	1	(3/2 <sup>-</sup> )	0.55	0.038			
3.25	1	(3/2 <sup>-</sup> )	2.08	0.14			
3.77	{(3) (5)}	(5/2 <sup>-</sup> ) (9/2 <sup>-</sup> )	1.18	{0.98 0.55}			
3.86	{(1) (5) (6)}	(1/2 <sup>-</sup> ) (9/2 <sup>-</sup> ) (13/2 <sup>+</sup> )	1.11	{0.93 0.18 0.09}			
4.05	{(1) (5) (6)}	(1/2 <sup>-</sup> ) (9/2 <sup>-</sup> ) (13/2 <sup>+</sup> )	0.84	{0.68 0.13 0.13}			
4.11	{(1) (5) (6)}	(1/2 <sup>-</sup> ) (9/2 <sup>-</sup> ) (13/2 <sup>+</sup> )	0.59	{0.50 0.09 0.05}			
4.19	{(1) (5) (6)}	(1/2 <sup>-</sup> ) (9/2 <sup>-</sup> ) (13/2 <sup>+</sup> )	1.05	{0.92 0.11 0.09}			
4.34	{(1) (5) (6)}	(1/2 <sup>-</sup> ) (9/2 <sup>-</sup> ) (13/2 <sup>+</sup> )	2.15	{1.73 0.33 0.33}			
4.44	{(1) (5) (6)}	(1/2 <sup>-</sup> ) (9/2 <sup>-</sup> ) (13/2 <sup>+</sup> )	1.81	{1.58 0.20 0.15}			

TABLE VI. Spectroscopic data from  $\text{Te}^{126}(d,p)\text{Te}^{127}$  reactions. See also the caption for Table IV.

Excit. energy (MeV)	$l_n$	$J^\pi$	$\sigma(\theta_0)$ (mb/sr)		Known (Ref. 14)		
			$S_p$	Excit. energy	$J^\pi$	$S_p/S_t$	
0.00	2	$3/2^+$	2.56	0.41	0	$(3/2^+)$	0.64
0.07	{0 (5)	$1/2^+$	2.17	1.93	0.48	0.887	$(11/2^-)$
		$(11/2^-)$		0.32	0.45		
0.63	{0 (2)	$1/2^+$	0.17	0.11	0.026	0.46	
0.77	{2 (5)	$(5/2^+)$	0.17	0.013	0.011	0.71	?
		$(5/2^+)$		0.90	0.079	0.77	
1.14	2	$(5/2^+)$		0.21	0.017		0.25
1.30	{1 (2)	$(3/2^-)$	0.11	0.035	0.003		0.12
		$(3/2^+)$		0.07	0.008		
1.39	{0 (2)	$1/2^+$	0.22	0.17	0.026		
		$(3/2^+)$		0.10	0.012		
1.55	{1 (2)	$(3/2^-)$	0.18	0.06	0.005		
		$(3/2^+)$		0.11	0.014		
1.69	{2 (1)	$(3/2^+)$	0.10	0.05	0.005		
		$(3/2^-)$		0.03	0.003		
1.82	{1 (5)	$(3/2^-)$	0.08	0.07	0.006		
		$(9/2^-)$		0.01	0.010		
1.91	{1 (5)	$(3/2^-)$	0.17	0.11	0.09		
		$(9/2^-)$		0.07	0.06		
2.01	3	$7/2^-$		1.36	0.15		
2.12	3	$7/2^-$		1.37	0.15		
2.20	{1 (5)	$(3/2^-)$	1.76	1.56	0.12		
		$(9/2^-)$		0.21	0.16		
2.30	{1 (5)	$(3/2^-)$	0.56	0.54	0.032		
		$(9/2^-)$		0.15	0.11		
2.45	{1 (5)	$(3/2^-)$	0.76	0.68	0.050		
		$(9/2^-)$		0.09	0.033		
2.56	...	...		0.24			
2.61	1	$(3/2^-)$		0.17	0.012		
2.77	3	$(7/2^-)$		0.21	0.017		
2.82	3	$(7/2^-)$		0.33	0.028		
2.92	1	$(3/2^-)$		0.26	0.017		
3.03	...	...		0.15			
3.12	{1 (3)	$(3/2^-)$	0.53	0.48	0.024		
		$(7/2^-)$		0.14	0.021		
3.32	{3 (3)	$(7/2^-)$	0.53	0.45	0.068		
		$(3/2^-)$		0.85	0.054		
3.40	1	$(3/2^-)$		1.62	0.10		
3.54	1	$(3/2^-)$		1.05	0.065		
3.74	1	$(3/2^-)$		1.06	0.064		
3.84	{1 (5) (6)	$(3/2^-)$	1.21	0.13	0.07		
		$(13/2^+)$		0.10	0.10		
3.91	3	$(5/2^-)$		0.69	0.054		
4.14	1	$(1/2^-)$		1.07	0.126		
4.22	1	$(1/2^-)$		0.84	0.098		
4.76	{3 (1)	$(5/2^-)$	1.07	1.73	0.11		
		$(1/2^-)$		0.94	0.122		
4.88	{5 (6)	$(9/2^-)$	1.07	0.12	0.043		
		$(13/2^+)$		0.08	0.070		
5.37	3	$(5/2^-)$		2.46	0.27		

In  $\text{Te}^{125}$  this problem has become so acute that nothing could be analyzed in the regions that are seen blank in the diagram.  $\text{Te}^{131}$  has three holes in a closed shell of 82 neutrons and therefore the spectrum is not expected to be very complicated as is seen in Fig. 9. But the complexity of the neutron spectra is expected to increase as one moves further from the closed neutron shell. It

TABLE VII. Spectroscopic data from  $\text{Te}^{124}(d,p)\text{Te}^{125}$  reactions. See also the caption for Table IV.

Excit. energy (MeV)	$l_n$	$J^\pi$	$\sigma(\theta_0)$ (mb/sr)		Known (Ref. 14)		
			$S_p$	Excit. energy	$J^\pi$	$S_p/S_t$	
0.00	{0 (2)	$1/2^+$	1.24	0.50	0.075	0.00	$1/2^+$
		$(3/2^+)$		1.50	0.24	0.035	$3/2^+$
0.64	2	$(5/2^+)$	0.45	0.037	0.63	$5/2^+$	0.18
0.70	2	$(5/2^+)$	0.18	0.015	0.64	$7/2^+$	
0.77	{2 (4)	$(5/2^+)$	0.11	0.07	0.006	0.67	$5/2^+$
		$(7/2^+)$		0.075	0.043		
1.81	2	$(3/2^+)$		0.15	0.014		
1.91	2	$(3/2^+)$		0.36	0.034		
1.98	{1 (2)	$(3/2^-)$	0.17	0.12	0.009		
		$(3/2^+)$		0.11	0.011		
2.03	{1 (2)	$(3/2^-)$	0.25	0.17	0.013		
		$(3/2^+)$		0.14	0.014		
2.11	(1)	$(3/2^-)$		0.64	0.05		

TABLE VIII. Spectroscopic data from  $\text{Te}^{125}(d,p)\text{Te}^{126}$  reactions. See also the caption for Table IV.  $j_n$  is the total angular momentum (orbital + spin) of the captured neutron. The details of obtaining the spectroscopic factors in these reactions are explained in the text.

Excit. energy (MeV)	$l_n$	$j_n$	$J^\pi$	$\sigma(\theta_0)$ (mb/sr)		Known (Ref. 14*)	
				$S_p$	Excit. energy	$J^\pi$	
0.00	0	$1/2^+$	$0^+$	0.94	0.085	0.00	$0^+$
0.69	(2)	$(3/2^+)$	$(2^+)$	0.081	0.068	0.67	$2^+$
1.43	(2)	$(5/2^+)$	$(2^+)$	0.061	0.022	1.42	$2^+$
1.53	(2)	$(5/2^+)$	$(2^+,3^+)$	0.042		...	...
						2.19	$(3^-)$
2.21	(2)	$(3/2^+)$	$(1^+,2^+)$	0.27		2.23	
2.43	{0 (2)	$1/2^+$	$0^+$	0.35	0.026	0.17	2.40
						$(3/2^+)$	$(1^+,2^+)$
2.53	2	$(3/2^+)$	$(1^+,2^+)$	0.19		2.51	...
2.60	0	$1/2^+$	$0^+$	0.32	0.049		
2.69	{1 (2)	$(3/2^-)$	$(1^-)$	0.24	0.025	0.15	2.74
						$(3/2^+)$	$(1^+,2^+)$
2.84	...	...		0.79		2.86	
3.34	...	...		0.23			
4.03	...	...		0.29			
4.56	...	...		0.40			
4.69	...	...		0.67			
4.93	...	...		0.61			
5.00	...	...		0.54			
5.13	...	...		0.46			

\* Also, G. C. Pramila (private communication).

is because of these considerations that (i) the occupation numbers of the quasiparticle states in  $\text{Te}^{131}$  were treated as standard to renormalize those in other isotopes and (ii) the occupation numbers of the states in the next major shell cannot be trusted for any important results or pairing theory calculations while the positions of the centers of gravity of the various single-particle states

TABLE IX. Spectroscopic data from  $\text{Te}^{130}(d,t)\text{Te}^{129}$  reactions. The spin assignments listed here are taken from the  $\text{Te}^{128}(d,p)\text{Te}^{129}$  reactions.  $\sigma_{av}$  is the average of the experimental cross sections obtained from the  $(d,t)$  reaction spectra at  $45^\circ$  and  $60^\circ$ . Other details of obtaining these data are described in the text.

Excit. energy (MeV)	$J^\pi$	$\sigma_{av}$ (mb/sr)	$S_t$	Excit. energy from $(d,p)$
0.00	$3/2^+$	1.72	0.73	0.00
0.10	$(11/2^-)$	0.58	0.57	0.11
0.18	$1/2^+$	2.48	0.65	0.17
0.25		0.03		
0.36		0.054		
0.42		0.12		
0.55		0.044		
0.73		0.054		
0.80		0.069		
0.87		0.03		
0.96	$(5/2^+)$	0.94	0.29	0.97
1.11		0.15		
1.27	{ $(7/2^+)$ $(5/2^+)$	0.51		1.28
1.40		0.098		
1.49		0.044		
1.64		0.49		
1.76		0.16		
1.85		0.059		
1.89		0.064		
2.09	$(7/2^-)$	0.054		2.10
2.24	$(7/2^-)$	0.054		2.22
2.34	$(7/2^-)$	0.11		2.36



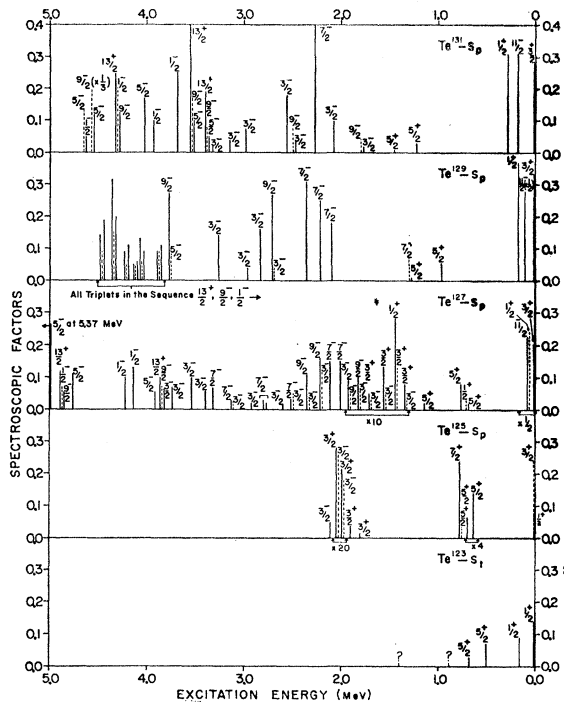


FIG. 9. The energy spectra of protons from  $(d,p)$  reactions on  $Te^{130}$ ,  $Te^{128}$ ,  $Te^{126}$ , and  $Te^{124}$  and the energy spectrum of tritons from  $(d,t)$  reactions on  $Te^{124}$ .  $S_p$  and  $S_t$  are spectroscopic factors from  $(d,p)$  and  $(d,t)$  reactions, respectively. The diagram is a plot of spectroscopic factors against excitation energy. All close doublets or triplets that have a broken line as a member represent unresolved states. The short lines beneath the question marks in  $Te^{123}$  do not represent spectroscopic factors but merely denote positions of some states of  $Te^{123}$ .

may still be reliable as long as no components of the quasiparticle state multiplet are not out of the range of investigation in the present work. This possibility of some components falling outside of the range of energy

TABLE X. Spectroscopic data from  $Te^{128}(d,t)Te^{127}$  reactions. See also the caption for Table IX.

Excit. energy (MeV)	$J^\pi$	$\sigma_{av}$ (mb/sr)	$S_t$	Excit. energy from $(d,p)$
0.00	$3/2^+$	1.35	0.64	0.00
0.06	$\{1/2^+$	2.84	0.61	0.07
0.48	$(11/2^-)$			
0.67	$\{1/2^+$	0.10	0.31	0.63
0.77	$(5/2^+)$			
0.92	$(5/2^+)$	0.26	0.14	1.14
1.12	$(5/2^+)$	0.45	0.14	1.14
1.28	$\{(3/2^-)$	0.24	0.14	1.30
1.36	$(3/2^+)$			
1.41	$(1/2^+)$	0.80	0.14	1.39
1.78	$(3/2^+)$			
1.85	$\{(3/2^-)$	0.07	0.11	1.82
1.92	$(9/2^-)$			
2.08	$(7/2^-)$	0.12	0.12	2.12

TABLE XI. Spectroscopic data from  $Te^{126}(d,t)Te^{125}$  reactions. See also the caption for Table IX.

Excit. energy (MeV)	$J^\pi$	$\sigma_{av}$ (mb/sr)	$S_t$	Excit. energy from $(d,p)$
0.00	$1/2^+$	1.29	0.41	0.0
0.03	$(3/2^+)$	1.19	0.60	
0.14	$(11/2^-)$	0.38	0.48	
0.46	$(5/2^+)$	0.13		0.64
0.67	$(5/2^+)$	0.78	0.27	
0.80	$\{(5/2^+)$	0.10		0.77
	$(7/2^+)$			
1.06		0.42		
1.14		0.31		
1.28		0.25		
1.46		0.18		
1.61		0.06		

investigated here has been indicated in Table III by putting a symbol  $\gtrsim$  in front of the energies (quasi- and single particle) of some of the states. This can be further checked by a closer examination of Fig. 9. Figure 10 presents all the single-quasiparticle states that were observed almost completely (this statement implies the hope that in these states the levels that are missed, causing a low value of  $U_j^2$ , did not affect the position of the "center of gravity" of the state, the missed levels being symmetrically situated above the center of gravity of the state). A surprising feature of this figure is the

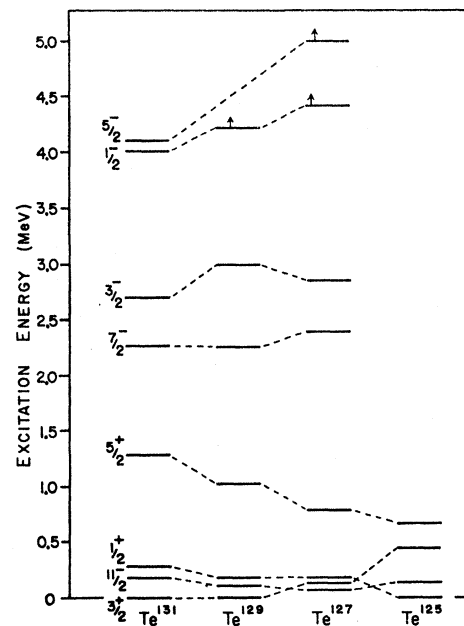


FIG. 10. The centers of gravity of the various single-quasiparticle states in the odd isotopes of Te are plotted against their mass numbers. Those states which are not shown in the diagram are believed to be partially missed. Obviously some high-energy components of the  $3/2^-$  state in  $Te^{127}$  have been missed. The arrow on some of the states means that the actual state probably lies a little higher than indicated.

low position of the  $\frac{3}{2}^-$  single-quasiparticle state in  $\text{Te}^{127}$ . Of course the spectrum of  $\text{Te}^{127}$  was very complex and it is probable that some high excitation energy components of the  $\frac{3}{2}^-$  state have been missed in a region crowded with several other states. Looking at the spectra in the neighboring (Fig. 9) isotopes it seems very unlikely that some higher excitation  $l_n=1$  states have been wrongly assigned to  $\frac{3}{2}^-$ .

*Te<sup>131</sup> via (d,p) reactions.* The results are listed in Table IV. Only the first two excited states were previously known.<sup>14</sup> All excited states up to 4.63 MeV have been assigned spins using the shell model. As Fig. 9 shows the ambiguity of assignment of spins between  $\frac{3}{2}^-$  and  $\frac{1}{2}^-$  is fairly well resolved [except for the states above 3 MeV (Fig. 6) which could be  $\frac{1}{2}^-$  though the assignments given in Fig. 9 are hoped to be more favored] as the two groups are  $\sim 1.3$  MeV apart which is close to the separation expected from Table I. The assignment of  $\frac{5}{2}^+$  to the states 1.22 and 1.46 is from systematics (see Figs. 4 and 9). The quality of the fits to the experimental angular distributions [Figs. 5(a) and 5(b)] is generally satisfactory except for the  $l_n=1$  angular distributions in the 3–4-MeV excitation energy region where the 30° points are consistently too low and the 50° points consistently too high. The  $l_n=5$  theoretical angular distribution is too steep as compared to the experimental distribution for the 0.18-MeV state. In Table II, it is evident that the numbers  $U_j^2$  of all the states in the next major shell have to be renormalized. But the fact that  $U_{3/2}^2$  is half as much as  $U_{1/2}^2$  may have in part to do with the filling of this subshell before the previous major shell is full.

*Te<sup>129</sup> via (d,p) and (d,t) reactions.* The results from these reactions are listed in Tables V and IX, respectively. In this case too only the first two excited states were previously known.<sup>14</sup> The evidence for the presence of a  $\frac{7}{2}^+$  at 1.28 MeV is uncertain as the angular distribution of this state can also be fitted to that for  $l_n=3$  (Fig. 6), but one does not expect a  $\frac{7}{2}^-$  in this region (see Fig. 9). The same remarks as in  $\text{Te}^{131}$  via (d,p) apply to the general quality of angular distribution fits and to the fits for the special cases of  $l_n=1$  and  $l_n=5$  [Figs. 6(a) and 6(b)]. The most interesting observation in Table IX is the set of states at 2.09, 2.24, and 2.34 MeV of excitation energy. The agreement with the energies of the states observed in (d,p) is good as usual within the limitations of experimental accuracy. These states are believed to be  $\frac{7}{2}^-$  both from (d,p) angular distributions and systematics (Fig. 9). The fact that these are seen in (d,t) reactions, though with low cross sections, suggests that the next major shell  $82 < N \leq 126$  is beginning to fill even before the previous major shell is completely full. If this is true, it is contrary to the shell model belief that the major shells fill sequentially.

<sup>14</sup> *Nuclear Data Sheets*, compiled by K. Way *et al.* (Printing and Publishing Office, National Academy of Sciences–National Research Council, Washington 25, D. C.).

The  $\frac{5}{2}^+$  spin assignments derive support from the ratio  $S_n/S_t$  as explained earlier in the text.

*Te<sup>127</sup> via (d,p) and (d,t) reactions.* Only the first two states were previously known<sup>14</sup> (see Tables VI and X). Despite the complexity of the (d,p) spectra, the angular distribution fits [Fig. 7(a) and 7(b)] are quite good but the  $U_j^2$  for the single-particle states of the next major shell cannot be trusted as several states may have been missed. The cross section for the 11/2<sup>-</sup> state which is seen mixed with  $\frac{1}{2}^+$  at 0.06 MeV in (d,t) spectra, is obtained by interpolation between the neighboring isotopes. The 1.39-MeV state seen in (d,p) reactions is probably resolved into 1.36 and 1.41 in (d,t) reactions. From the ratio of (d,t) cross sections at 45° and 60°, the 1.36-MeV state seems to be  $\frac{1}{2}^+$  and therefore the 1.41-MeV state must be  $\frac{3}{2}^+$ . Its ratio of (d,t) cross sections at 45° and 60° agrees with this assignment. These ratios of cross sections were taken from the (d,t) angular distributions from Sn isotopes measured by Cohen and Price.<sup>2</sup> Once again states from the next major shell are seen excited in (d,t) reactions which supports the conclusion stated earlier.

*Te<sup>125</sup> via (d,p) and (d,t) reactions.* The results of analyses on these spectra are listed in Tables VII and XI. The splitting of the single-particle states is the largest in these spectra resulting in too much interference and very low cross sections for individual states. As a result most of the states could not be identified. Assignments of some of the low-lying levels up to 0.7 MeV which were previously known<sup>14</sup> have been verified (see Table VII), and some new assignments have been made. The ground state and the 0.03-MeV states are seen resolved in (d,t) reactions. The spin assignment  $\frac{1}{2}^+$  to the ground state, which is previously known,<sup>14</sup> is supported by the ratio of (d,t) cross sections at 45° and 60° as explained earlier. The states at 0.14 MeV and 0.46 MeV (Table XI) which have been missed in (d,p) reactions are known to be 11/2<sup>-</sup> and  $\frac{5}{2}^+$  from previous work.<sup>14</sup>

*Te<sup>123</sup> via (d,t) reactions.* The results of analyses of these reactions are given in Table XII. The spin and parity assignments are made on the basis of systematics (see Fig. 9) or the ratio of cross sections at 45° and 60° as mentioned previously.

TABLE XII. Spectroscopic data from  $\text{Te}^{124}(d,t)\text{Te}^{123}$  reactions. The  $J^\pi$  possibilities listed here are derived from systematics and  $\sigma_{45^\circ}/\sigma_{60^\circ}$  ratios. See also the caption for Table IX.

Excit. energy (MeV)	$J^\pi$	$\sigma_{av}$ (mb/sr)	$S_t$	Known (Ref. 14)	
				$J^\pi$	Excit. energy
0.00	(1/2 <sup>+</sup> )	0.45	0.14	1/2 <sup>+</sup>	0.0
0.16	(1/2 <sup>+</sup> )	0.29	0.09	1/2 <sup>+</sup>	0.159
0.50	(5/2 <sup>+</sup> )	0.19	0.07		0.502
0.67	(5/2 <sup>+</sup> )	0.089	0.03		0.69
0.89		0.32			
1.39		0.14			

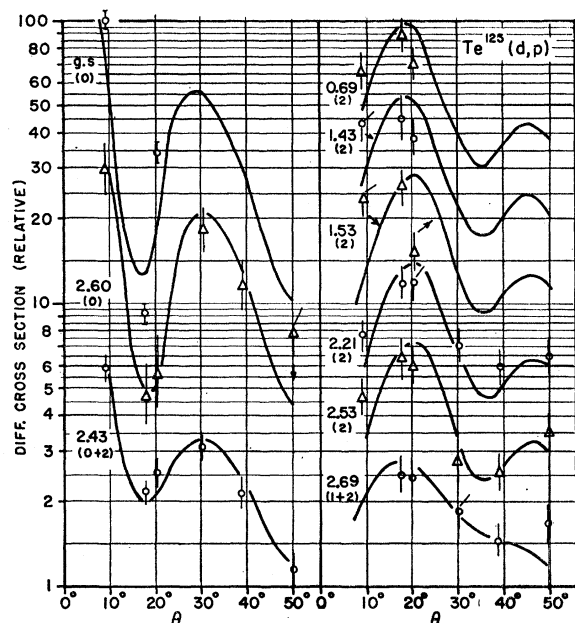


FIG. 11. Angular distributions of the proton groups leading to the states of  $\text{Te}^{126}$ . See also the caption for Fig. 5.

### B. Spectroscopy of the Even Isotopes

$\text{Te}^{126}$  via  $(d,p)$  reactions. The angular distributions of the first four states are incomplete because of an accident but fortunately the spins and parities of three of them are previously known. The spin and parity assignments  $\frac{5}{2}^+$  for the captured neutrons (Table VIII) leading to the states 1.43 and 1.53 MeV of  $\text{Te}^{126}$  have been made on the basis of systematics with neighboring odd nuclei (see Fig. 9) taking into account the pairing energy of  $\sim 0.6$  MeV since  $\frac{3}{2}^+$  and  $\frac{1}{2}^+$  states of the transferred neutron are within 70 keV of each other in both  $\text{Te}^{127}$  and  $\text{Te}^{125}$  while these are almost  $\sim 0.7$  MeV apart here. The angular distributions of states beyond 2.69 MeV of excitation energy are incomplete because of their difficult identification at all angles. Two  $0^+$  states in addition to the ground state are noticed; the one at 2.43 is mixed with another state corresponding to an orbital angular momentum transfer of 2 units while the other at 2.60 is pure. The angular distributions in both cases are unmistakable (see Fig. 11). The details of obtaining the spectroscopic factors in these reactions have been explained earlier.

$\text{Te}^{124}$  via  $(d,t)$  reactions. States up to 3.89 MeV have been observed (Table XIII). The spins and parities of the picked up neutron have been assigned from systematics.

The results for the even isotopes are summarized in Fig. 12. The correspondence between the states of  $\text{Te}^{124}$  and  $\text{Te}^{126}$  is often clear and may be used for additional spin and parity assignments in the absence of any other information.

TABLE XIII. Spectroscopic data from  $\text{Te}^{125}(d,t)\text{Te}^{124}$  reactions. The total angular momentum possibilities  $j_n$ , for the picked up neutron are derived from systematics and  $\sigma_{45^\circ}/\sigma_{60^\circ}$  ratios while the  $J^\pi$  possibilities are derived from simple angular momentum coupling considerations. See also the caption for Table IX.

Excit. energy (MeV)	$j_n$	$J^\pi$	$\sigma_{av}$ (mb/sr)	Known (Ref. 14)	
				Excit. energy	$J^\pi$
0.00	$(1/2^+)$	$(0^+)$	0.49	0.0	$0^+$
0.61	$(3/2^+)$	$(2^+)$	0.15	0.603	$2^+$
1.32	$(5/2^+, 7/2^+)$	$(2^+, 4^+)$	0.06	1.326	$2^+$
2.31			0.36	2.295	$3^-$
2.44			0.07		
2.53			0.49		
2.59			0.15		
2.78			0.18	2.745	$(1 \pm, 2 \pm)$
2.84			0.10	2.865	$(2, 3)^-$
3.12			0.09		
3.16			0.07		
3.20			0.10		
3.28			0.08		
3.43			0.10		
3.58			0.10		
3.67			0.12		
3.75			0.06		
3.81			0.21		
3.89			0.19		

### IV. COMPARISON WITH THE SPECTRA OF Sn ISOTOPES

A comparison of the detailed low-lying neutron level spectra in the isotones of Sn and Te is made in Fig. 13 with a view to verifying the hope that the spectra of such isotonic pairs do not look very different. It is immediately apparent that such hopes are belied as the spectra of isotones look considerably different. Te isotones have more complex spectra than their Sn counterparts. Aside from this the ordering of levels is quite different too. For a more meaningful comparison, the spectra of the centers of gravity of states of the same spin and parity of the isotonic pairs  $\text{Te}^{127}$ ,  $\text{Sn}^{125}$  and  $\text{Te}^{125}$ ,  $\text{Sn}^{123}$  have been drawn on the same scale in Fig. 14. It is once again clear that the spectra of isotones do not agree. While the single-quasiparticle states of the Te

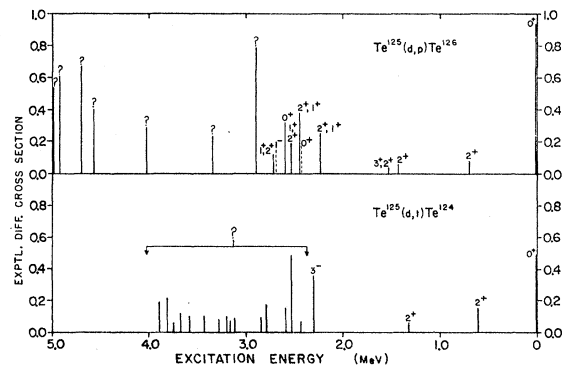


FIG. 12. The energy spectra of protons and tritons from  $\text{Te}^{125}(d,p)\text{Te}^{126}$  and  $\text{Te}^{125}(d,t)\text{Te}^{124}$  reactions. The plots are experimental differential cross section against excitation energy. Other details are explained in the text.

isotopes are confined to within 0.8 MeV from the ground state, the Sn spectra go up to 1.4 MeV. This shows that the addition of two protons to a closed shell core of 50 protons (in Sn isotopes) makes a great difference in the neutron spectra. A similar comparison among the members of Sn and Cd isotonic pairs by Cohen and Price<sup>2</sup> showed similar results.

V. REACTION Q VALUES

Q values of (d,p) and (d,t) reactions on the isotopes 130, 128, 126, 125, and 124 of Te have been calculated and compared with previously known values from Ref.

TABLE XIV. Reaction Q values. The second number in Columns 3 and 4 is the quoted uncertainty in the Q values.

Target	Reaction	Q (MeV)	
		This work	Ref. 15
124	(d,p)	4.33, 0.1	4.29, 0.4
	(d,t)	-3.37, 0.1	-3.09, 0.43
125	(d,p)	6.80, 0.1	6.76, 0.4
	(d,t)	-0.55, 0.1	-0.26, 0.4
126	(d,p)	4.00, 0.1	4.22, 0.36
	(d,t)	-3.08, 0.1	-2.73, 0.4
128	(d,p)	3.79, 0.1	4.28, 0.52
	(d,t)	-2.81, 0.1	-2.36, 0.5
130	(d,p)	3.61, 0.1	4.06, 0.38
	(d,t)	-2.54, 0.1	-1.67, 0.44

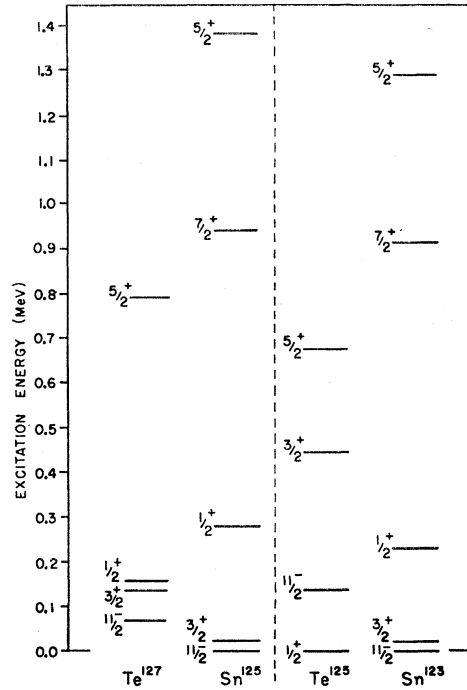


Fig. 14. A comparison of the single-quasiparticle neutron energy spectra in the isotonic pairs Sn<sup>123</sup>, Te<sup>125</sup> and Sn<sup>125</sup>, Te<sup>127</sup>.

15. Since the incident deuteron energy is uncertain within 100 keV, the absolute Q values may be uncertain by about the same amount while the relative Q values among neighboring isotopes should be accurate to ~40 keV. The results are listed in Table XIV. The agreement with the values of Ref. 15 is good within experimental uncertainties.

ACKNOWLEDGMENTS

The author is grateful to Professor B. L. Cohen for suggesting the problem and for continuous advice and encouragement throughout this work. The help of Dr. Satchler at Oak Ridge in carrying through the DWBA calculations carefully is thankfully acknowledged. Helpful discussions with R. H. Fulmer and Professor R. M. Drisko are greatly appreciated. Thanks are also due to George Fodor of this laboratory for preparing the targets, to J. D. Francesco and R. E. Leonard for help in taking data, and Addie Trent and co-workers for scanning the plates and plotting the data.

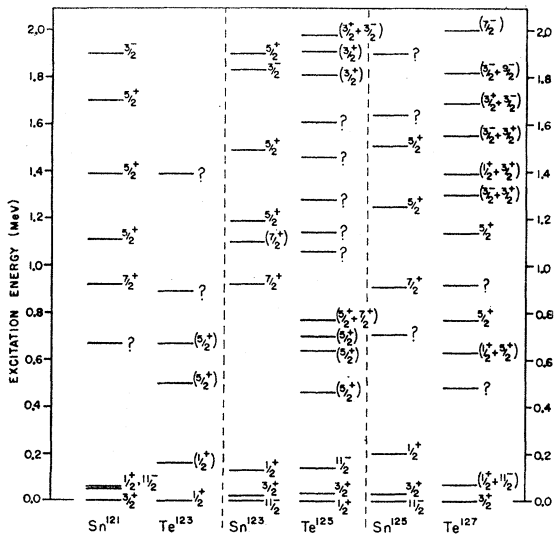


Fig. 13. A comparison of the detailed neutron energy spectra in the isotonic pairs Sn<sup>121</sup>, Te<sup>123</sup>; Sn<sup>123</sup>, Te<sup>125</sup>; and Sn<sup>125</sup>, Te<sup>127</sup>.

<sup>15</sup> "Tables of Reaction Q Values," University of California Radiation Laboratory Report No. UCRL 5419 (unpublished).